JCI insight

Inhibiting Triggering Receptor Expressed on Myeloid Cells-1 signaling to ameliorate skin fibrosis

Swarna Bale, … , Swati Bhattacharyya, John Varga

JCI Insight. 2024. https://doi.org/10.1172/jci.insight.176319.

Research In-Press Preview Infectious disease

Graphical abstract

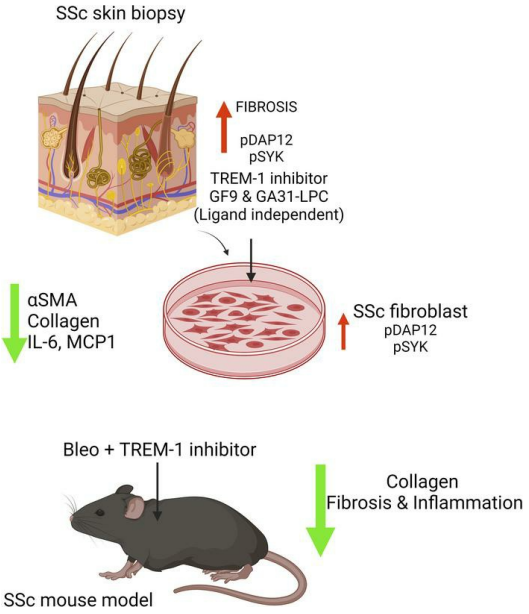

Inhibiting Triggering Receptor Expressed on Myeloid Cells-1 signaling to ameliorate skin fibrosis

Authors

Swarna Bale[1], Priyanka Verma[1], Bharath Yalavarthi[1], Matija Bajželj[1], Syed Hasan[1], Jenna Silverman[1], Katherine Broderick[1], Kris Shah[1], Timothy Hamill[1], Dinesh Khanna[1], Alexander Sigalov[2]*, Swati Bhattacharyya[1]*, John Varga[1]*

Key words: Fibrosis, systemic sclerosis, fibroblast, myofibroblast, TREM-1, GF9, GA31, lipopeptide complex

Affiliations

[1]Michigan Scleroderma Program, Division of Rheumatology, Department of Internal Medicine, University of Michigan, Ann Arbor, Michigan, United States of America

[2]SignaBlok, Inc., Shrewsbury, Massachusetts, United States of America

Swarna Bale[1] and Priyanka Verma[1], contributed equally

North Campus Research Complex Building 20-1880, 2800 Plymouth Rd, Ann Arbor, MI 48109,USA. Phone: 734-936- 6665; Email: vargaj@med.umich.edu (JV). Phone: 708-263-7733; Email: bhattasw@med.umich.edu (S Bhattacharyya). Phone: 203-505-3807; Email: sigalov@signablok.com (A Sigalov).

GRAPHICAL ABSTRACT

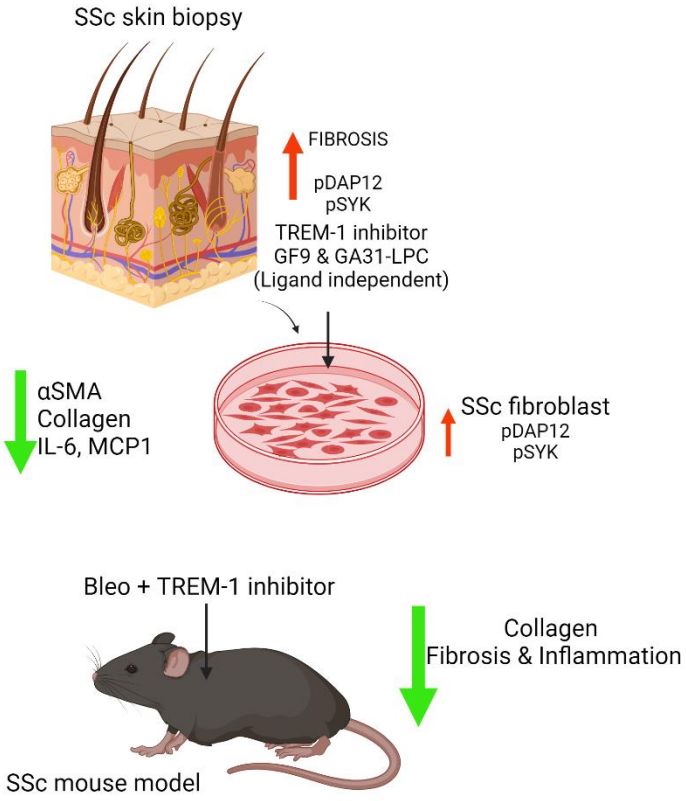

Created in BioRender.com

ABSTRACT

Systemic sclerosis (SSc) is characterized by immune system failure, vascular insult, autoimmunity, and tissue fibrosis. Transforming growth factor-beta (TGF-β) is a crucial mediator of persistent myofibroblast activation and aberrant extracellular matrix production in SSc. The factors responsible for this are unknown. By amplifying pattern recognition receptor signaling, Triggering Receptor Expressed on Myeloid Cells 1 (TREM-1) is implicated in multiple inflammatory conditions. In this study, we used novel ligand-independent TREM-1 inhibitors in order to investigate the pathogenic role of TREM-1 in SSc, using preclinical models of fibrosis, and explanted SSc skin fibroblasts. Selective pharmacological TREM-1 blockade prevented and reversed skin fibrosis induced by bleomycin in mice and mitigated constitutive collagen synthesis and myofibroblast features in SSc fibroblasts in vitro. Our results implicate aberrantly activated TREM-1 signaling in SSc pathogenesis, identify a unique approach to TREM-1 blockade, and suggest a potential therapeutic benefit for TREM-1 inhibition.

INTRODUCTION

Fibrosis that affects multiple organs is the hallmark sign of systemic sclerosis (SSc), and lacks effective therapy (1, 2). Fibrosis in SSc is associated with high mortality (3-5). Numerous intracellular signaling pathways are implicated as drivers of SSc fibrosis, but the nature of their continuing dysregulation in pathological inflammation and fibrosis remains poorly understood. Recent studies have uncovered an essential role for innate immunity in the pathogenesis of SSc (6). As a component of the innate immune system, the cellular receptor Triggering Receptor Expressed on Myeloid Cells 1 (TREM-1) is expressed on neutrophils, monocytes, macrophages, and endothelial cells (7, 8). Endogenous ligands for TREM-1 include high mobility group box 1 (HMGB1), Hsp70 (heat shock protein 70), peptidoglycan recognition protein 1 (PGLYRP), and extracellular cold-inducible RNA-binding protein (eCIRP1) (9). Activation of TREM-1 leads to phosphorylation of its signaling partner DNA-activating protein of 12 kDa (DAP12), which induces cytokine and chemokine production (10, 11). However, the expression, role and mechanisms of TREM-1 signaling in fibrosis in SSc are currently unknown (9, 12).

Upregulation of TREM-1 on immune cells is implicated in acute inflammation (7, 13), while sustained TREM-1 activation plays a crucial role in sepsis, arthritis, and colitis (11, 13-16). Notably, TREM-1 amplifies signaling from cellular pattern recognition receptors (PRR) such as Toll-like receptor 4 (TLR4), thus amplifying the inflammatory response (17, 18). In previous studies, we established an essential role for several extracellular matrix proteins as damage-associated molecular patterns (DAMPs) that function as endogenous ligands for TLR4 to drive sustained fibroblast activation underlying fibrosis progression in SSc (19, 20). In light of TREM-1's potential to interact with the TLR4 signaling pathways, we sought to explore the involvement of TREM-1 in SSc and the impact of TREM-1 inhibition in preclinical models of fibrosis.

There has been substantial effort to develop therapeutic TREM-1 inhibitors. Currently available TREM-1 blockers, including inhibitory peptides LR12 and M3 (21-25), the small molecule VJDT (26), and an anti-TREM-1 antibody (27), are ligand-dependent inhibitors that block TREM-1 binding to its ligand(s) (28). At least five different molecules have been reported as putative TREM-1 ligands (29). In the pathogenesis of TREM-1-linked inflammatory diseases, the expression of these molecules depends on disease pathogenesis, stage, and severity, which might affect the efficacy of ligand-dependent TREM-1 inhibitors. Importantly, despite promising results in disease models in small and large animals, and safety in humans (30-35), the first clinical TREM-1 blocker, LR12 peptide (Nangibotide), failed in a recent Phase IIb sepsis trial (25).

In the present study, we sought to characterize the involvement of TREM-1 in SSc. We used unique TREM-1 inhibitors to determine the impact of TREM-1 in preclinical disease models. These inhibitors were created based on the TREM-1 inhibitory peptide sequence GF9 (reviewed in (28). The free peptide GF9 and GA31 peptide formulated in macrophage-targeted lipopeptide complexes (GA31-LPC) employ a ligand-independent mechanism to disrupt protein-protein interactions between TREM-1 and DAP-12 at the membrane (28). Systemically administered GF9 functions as a "pan-TREM-1" blocker on all TREM1-expressing cells (neutrophils, monocytes, macrophages), while GA31-LPC blocks TREM-1 primarily on macrophages (28). Treatment with GF9 and GA31-LPC were previously shown to suppress systemic and local inflammation and ameliorate disease in animal models of rheumatoid arthritis, alcoholic liver disease, retinopathy, and cancer (36-39).

Here, we demonstrate that TREM-1 signaling was activated in SSc skin biopsies, and its inhibition mitigated constitutive collagen synthesis and the myofibroblasts phenotype in explanted SSc fibroblasts. Furthermore, ligand-independent selective TREM-1 blockade prevented and reversed

bleomycin-induced fibrosis in mice. Together, these results implicate aberrant TREM-1 signaling in SSc,and provide a rationale for further exploring selective TREM-1 targeting as a distinct therapeutic strategy.

RESULTS

TREM-1 inhibitors treated at early time point prevented bleomycin induced responses.

In this study, we used first time TREM-1 inhibitors GF9 and GA31-LPC (34-37) in a preclinical disease model of fibrosis. Eight-week-old female C57BL/6J mice were injected with bleomycin daily subcutaneously (s.c.) for one-week (5 days/week), concurrently with vehicle or GF9 (25 mg/kg) or GA31-LPC (13 mg/kg) given by daily intraperitoneal (i.p.) injections (5 days/week). Mice were sacrificed on day 8. Masson's trichrome staining of skin from mice treated with bleomycin, compared to vehicle-treated mice, showed decreased thickness of the cutaneous white adipose tissue (DWAT), associated with increased dermal thickness (Fig.1A). Dramatic bleomycin-induced loss of DWAT was substantially attenuated by treatment of the mice with GF9 or GA31-LPC (Fig. 1A). Loss of DWAT was further demonstrated using perilipin immunostaining (Fig.1C). Pharmacological TREM-1 blockade attenuated the increase in inflammatory cytokines including *Mcp1* and *Il6* (Fig. 1B). We observed no significant difference in dermal thickness and skin procollagen I levels with TREM- 1 inhibitor treatment at this early timepoint (Fig. 1C). We investigated the effect of GF9 and GA31-LPC on accumulation of ASMA-positive interstitial myofibroblasts and phospho-DAP12 (a marker for TREM1 activation) and CD45-positive leukocytes. Interestingly, 7 days of GF9 and GA31-LPC treatment decreased accumulation of ASMA-positive myofibroblasts ($p=0.0057$ and $p=0.012$) (Fig 1D), as well as phospho-DAP12- and CD45-positive leukocytes (Suppl. Fig. 1A, 1B).

TREM-1 inhibition concomitant with bleomycin administration prevented skin fibrosis

We next examined the effect of treatment with GF9 and GA31-LPC for 21 days. Treated mice showed no significant weight loss, and treatment was well tolerated with no behavioral changes or overt signs of toxicity. Bleomycin-treated mice showed increased dermal collagen accumulation, enhanced dermal thickness, and loss of DWAT, compared to PBS treated mice (Fig. 2A). Concurrent GF9 or GA31-LPC treatment resulted in reduced collagen deposition and dermal thickness and restored DWAT compared to bleomycin-treated mice (Fig. 2A, B). When compared to early timepoints, the skin at 22 days of bleomycin treatment demonstrates increased numbers of ASMA-positive interstitial myofibroblasts, which was attenuated in mice with TREM-1 inhibitors administered concomitantly with bleomycin (Fig. 2C). Immunolabelling indicated a marked reduction in the numbers of CD45- leukocytes and CD11b-positive (pan myeloid marker), but no significant changes in T cell accumulation, in the dermis from mice treated with TREM-1 inhibitors. (Suppl. Fig. 2 and Suppl. Fig. 4).

Treatment with GF9 and GA31-LPC attenuated established skin fibrosis

To evaluate the effect of TREM-1 inhibition in the therapeutic approach, we initiated TREM1 inhibitor treatment on day 15 following the start of bleomycin, when skin fibrosis is already established (40). Analysis of the lesional skin showed that treatment with GF9 or GA31-LPC attenuated the bleomycin-induced increase in dermal thickness and collagen accumulation (Fig. 3A, B), and restored DWAT. Chronic administration of GF9 and GA31-LPC in these experiments appeared to be well tolerated.

TREM-1 signaling is activated in SSc skin biopsies.

To characterize TREM-1 activity in SSc, we determined levels of phosphorylated Syk, a marker of TREM-1 activation (41), in the skin. Immunolabelling of skin biopsies indicated significantly higher levels of phosphor-Syk ($p=0.004$), accompanied by increased number of ASMA-posotive interstitial cells ($p=0.0081$), in SSc skin biopsies compared to healthy controls, while there was no significant difference in TREM-1 levels (Fig. 4A). Further, levels of the TREM-1 activation target DAP12 was elevated in explanted SSc compared to healthy skin fibroblasts (Suppl. Fig. 3A). To investigate the effect of TREM-1 on explanted fibroblasts in vitro, confluent SSc skin fibroblasts were incubated in media with GF9 (10 μM) for 24 h. GF9 treatment was associated with substantial downregulation of mRNA levels of COL1A1 and ACTA2, as well as inflammatory cytokines MCP1 and IL-6 (Fig. 4B). Importantly, GF9 reduced the production of collagen I and cellular levels of ASMA, which was accompanied by a reduction in cellular phosphor-DAP12 and phospho-Syk levels (Fig. 4C, Suppl. Fig. 3B). Together, these results indicate a potent anti-fibrotic effect of TREM-1 inhibition in explanted SSc fibroblasts.

DISCUSSION

Fibrosis in SSc affects the skin and multiple internal organs (42). The pathogenesis of SSc is still poorly understood, but emerging evidence implicates dysregulated innate immune signaling (43). Patients with SSc have limited therapeutic options and unique therapeutic approaches are needed (44). TREM-1 is a widely expressed cellular receptor involved in innate immune signaling via the adaptor protein DAP12 (28). TREM-1 activation triggers phosphorylation and activation of the Src kinase Syk, resulting in Syk2 phosphorylation (41). The identity of TREM1 ligands remains incompletely established, and multiple putative endogenous ligands have been described (28). Blocking TREM-1 signaling has been explored as a potential approach to the treatment of

inflammation-associated disorders, including sepsis, rheumatoid arthritis, and retinal neovascularization, as well as cancer (13, 36, 37, 39, 45).

Soluble TREM-1 (sTREM-1) is a glycoprotein derived primarily from the proteolytic cleavage of membrane TREM-1, and is a biomarker for TREM1 activation. Levels of sTREM1 were elevated in patients with diffuse cutaneous SSc, and correlated with the severity of pulmonary fibrosis (30). These findings suggested that serum sTREM-1 could be a unique marker for disease severity (45). Furthermore, phospho-DAP12, the marker for TREM-1 activation was elevated in skin biopsies from patients with early stage SSc, as well as in the bleomycin-induced fibrosis model. Our present studies are the first to show that targeting TREM-1 using ligand-independent peptide inhibitors prevents and reverses pathological skin fibrosis in mice, and represents a potential anti-fibrotic strategy for the treatment of fibrosis in patients with SSc.

TREM-1 enhanced inflammatory response was observed in non-infectious disease models, including hemorrhagic shock, pancreatitis (acute inflammation), chronic inflammatory bowel diseases, and inflammatory arthritis (46-49). TREM-1-deficient mice displayed significantly reduced disease phenotype associated with reduced inflammatory infiltrates and diminished expression of pro-inflammatory cytokines, thus representing an attractive target for treating chronic inflammatory disorders (50). Such data are noteworthy in suggesting that TREM-1 also plays a regulatory role in influencing the disease outcome. Therefore, we pursued the inhibitors' anti-fibrotic effect in a preclinical fibrosis model. Treatment with GF9 and GA31-LPC exerted potent antifibrotic effects in mice, and mitigated the activated phenotype of SSc fibroblasts in vitro. Moreover, the inhibitors showed antifibrotic effects on established skin fibrosis model also. As expected, we have found downregulation of pDAP12 and the levels of inflammatory and profibrotic cytokines (MCP-1 and IL-6) and pan leukocyte marker CD45 and pan myeloid marker

(CD11b) in mice. While the ligands of TREM-1 are still unknown, it has been shown that TREM-1 activation amplifies inflammation and synergizes with TLR signaling (51). We have shown previously that expression of TLR4 and its endogenous damage-associated ligands (DAMPs) are elevated in SSc patients (6, 20). Ligand-induced TLR4 activation in stromal cells elicits potent stimulation of fibrotic gene expression, myofibroblast transformation and survival, thus contributing to fibrosis persistence and progression (19, 52). TREM-1 inhibitors prevented phosphorylation of cellular DAP12, an early event in both TLR4 and TREM-1 signaling. Therefore, blocking early events in fibrotic activation in stromal cells might represent a therapeutic approach to ameliorate fibrosis, and merits further investigation.

MATERIALS AND METHODS

Study approval

Biopsies were performed with written informed consent, as per protocols approved by the IRB for Human Studies at Northwestern University and the University of Michigan (00186936). Animal experiments were performed according to institutionally approved protocols and in compliance with the University Animal Care and Use Committee guidelines (PRO00011706).

Cell Culture and Reagents

The synthesis of the 9- and 31-mer TREM-1 inhibitory peptides, GFLSKSLVF (human TREM-1213-221, GF9) and GFLSKSLVFPLGEEM(O)RDRARAHVDALRTHLA (GA31), was described previously (39, 41, 53).

Primary cultures of fibroblasts were established by explanations from skin biopsies from patients with SSc. Low-passage fibroblasts grown in monolayers in plastic dishes were studied as previously described (54). All SSc fibroblasts are derived from patients with early-stage (< 3 years

from first non-Raynaud disease manifestation) disease. Clinical characteristics of subjects used in the study are listed in Table 1. All SSc skin biopsies were recruited from patients with diffuse cutaneous systemic sclerosis patients. Control skin biopsies were recruited from healthy subjects.

Sex as a biological variable

We used female mice (8-12 weeks old) in this study because they present more excellent fibrotic responses in the subcutaneous (s.c.) bleomycin model and SSc has more the solid female sex bias.

Model of dermal fibrosis

8-12-week-old female C57BL/6J mice (The Jackson Laboratory) received subcutaneous (s.c.) injections of bleomycin (10 mg/kg/day) or PBS daily for 10 days (5 days/week). GF9 (25 mg/kg) and GA31-LPC (13 mg/kg) daily intraperitoneal (i.p.) injections were started concurrently with bleomycin, and mice were sacrificed on day 8 or day 22. Another group of mice received GF9 and GA31-LPC injections starting at day 15 of bleomycin treatment and continuing until sacrifice at day 28. A third group of mice received PBS, and a fourth received bleomycin alone. Tissue collagen content was determined using Colorimetric Assay Kits (Biovision, Milpitas, CA).

Paraffin-embedded tissue sections (4 μm) were stained with Trichrome and analyzed as described (54). Skin collagen content was determined using hydroxyproline assays (Colorimetric Assay Kits, Biovision, Milpitas, CA). Total RNA isolated from mouse skin was reverse transcribed to cDNA using Supermix and analyzed by real-time qPCR (Applied Biosystems) on an Applied Biosystems 7500 Prism Sequence Detection System as described (4, 54).

Isolation and Analysis of RNA from SSc skin fibroblasts

At the end of the experiments, total RNA was isolated from SSc fibroblasts and reverse-transcribed to cDNA using Supermix (cDNA Synthesis Supermix; Quanta Biosciences, Gaithersburg, MD) as described (55). Amplification products (20 ng) were amplified using SYBR Green PCR Master Mix (Applied Biosystems, Foster City, CA) on an Applied Biosystems 7500 Prism Sequence Detection System. Primer sequences are listed in Table 2. Data were normalized to GAPDH RNA, and the fold change in samples was calculated (55).

Immunofluorescence confocal microscopy using SSc skin fibroblasts and skin biopsies

SSc fibroblasts seeded on 8-well Lab-Tek II chamber glass slides (Nalgene Nunc International, Naperville, IL) were incubated in serum-free DMEM with or without GF9 (10μM) for 24 h. Cells were then fixed, permeabilized, and incubated with antibodies to ASMA (Sigma, 1:500, A5228), type I collagen (Southern Biotechnology, 1:100, #1310-01) and p-Syk (CST 2710S), followed by Alexa-fluor-labelled secondary antibodies (Invitrogen) as described (55). For immunofluorescence, paraffin-embedded skin sections were incubated with antibodies to ASMA (Sigma, 1:100, A5228), pSyk (CST 2710S, 1:100), pDAP12 (ab314891, 1:100), CD45 (14-0451-82, 1:100), CD3(sc-20047; 1:100), , TREM-1 (Invitrogen PA5-47090, 1:100), Anti-CD11b antibody (Abcam AB133357, 1:100), procollagen I (Sigma, MAB1912 1:200) or perilipin (Abcam; ab61682) followed by appropriate secondary antibodies.

Nuclei were detected using DAPI. Slides were mounted, and immunofluorescence was evaluated in a blinded manner under a Nikon A1R laser scanning confocal microscope. Negative controls stained without primary antibodies were used to confirm immunostaining specificity.

Statistical Analysis

We used the Mann-Whitney U and Student's t-test (two-tailed) to compare two groups, with a p-value correction for multiple comparisons. We presented the data as means ± S.D unless otherwise indicated. We examined the differences among groups for statistical significance using analysis of variance (ANOVA) followed by Sidak's correction. A p-value less than 0.05 was considered significant. We analyzed the data using the Graph Pad prism (Graph Pad Software version 8, Graph Pad Software Inc., CA).

Data availability

All the raw and processed data is stored in University of Michigan shared folder S:\Intmed_Rheum\Research\VSclero_Lab and are available upon request. All data point presented in the graphs are available in the supporting data file as a supplemental file.

AUTHOR CONTRIBUTIONS

S Bhattacharyya, JV, and AS conceptualized the study. S Bhattacharyya wrote the original draft of the manuscript, and JV and AS edited it. S Bale, BY, and SH performed mouse experiments and analysis. PV, KB, KS, and TH performed all other experiments and data analysis. DK provided skin fibroblasts. All the authors reviewed and edited the manuscript.

ACKNOWLEDGMENTS

We thank members of the University of Michigan (UMICH) sclerolab, and the UMICH Microscopy Core. We also thank the McClinchey Lab (Ann, Arbor, MI) for histology support. This work was supported by R43AR078110 (Alexander B. Sigalov, Principal investigator) from the National Institute of Arthritis and Musculoskeletal and Skin Diseases (NIAMS) of the National Institutes of Health.

CONFLICT OF INTEREST: Authors declare no conflict of interest.

REFERENCES

1. Volkmann ER, and Varga J. Emerging targets of disease-modifying therapy for systemic sclerosis. *Nat Rev Rheumatol.* 2019;15(4):208-24.
2. Bhattacharyya S, Wei J, and Varga J. Understanding fibrosis in systemic sclerosis: shifting paradigms, emerging opportunities. *Nat Rev Rheumatol.* 2011;8(1):42-54.
3. Pope JE, Denton CP, Johnson SR, Fernandez-Codina A, Hudson M, and Nevskaya T. State-of-the-art evidence in the treatment of systemic sclerosis. *Nat Rev Rheumatol.* 2023;19(4):212-26.
4. Bhattacharyya S, Kelley K, Melichian DS, Tamaki Z, Fang F, Su Y, et al. Toll-like receptor 4 signaling augments transforming growth factor-beta responses: a novel mechanism for maintaining and amplifying fibrosis in scleroderma. *Am J Pathol.* 2013;182(1):192-205.
5. Ebata S, Yoshizaki-Ogawa A, Sato S, and Yoshizaki A. New Era in Systemic Sclerosis Treatment: Recently Approved Therapeutics. *J Clin Med.* 2022;11(15).
6. Bale S, Verma P, Varga J, and Bhattacharyya S. Extracellular Matrix-Derived Damage-Associated Molecular Patterns (DAMP): Implications in Systemic Sclerosis and Fibrosis. *J Invest Dermatol.* 2023;143(10):1877-85.
7. Bouchon A, Dietrich J, and Colonna M. Cutting edge: inflammatory responses can be triggered by TREM-1, a novel receptor expressed on neutrophils and monocytes. *J Immunol.* 2000;164(10):4991-5.
8. Colonna M. The biology of TREM receptors. *Nat Rev Immunol.* 2023;23(9):580-94.
9. Tammaro A, Derive M, Gibot S, Leemans JC, Florquin S, and Dessing MC. TREM-1 and its potential ligands in non-infectious diseases: from biology to clinical perspectives. *Pharmacol Ther.* 2017;177:81-95.
10. Carrasco K, Boufenzer A, Jolly L, Le Cordier H, Wang G, Heck AJ, et al. TREM-1 multimerization is essential for its activation on monocytes and neutrophils. *Cell Mol Immunol.* 2019;16(5):460-72.
11. Chen X, Eksioglu EA, Carter JD, Fortenbery N, Donatelli SS, Zhou J, et al. Inactivation of DAP12 in PMN inhibits TREM1-mediated activation in rheumatoid arthritis. *PLoS One.* 2015;10(2):e0115116.
12. Denning NL, Aziz M, Murao A, Gurien SD, Ochani M, Prince JM, et al. Extracellular CIRP as an endogenous TREM-1 ligand to fuel inflammation in sepsis. *JCI Insight.* 2020;5(5).
13. Gibot S, Kolopp-Sarda MN, Bene MC, Bollaert PE, Lozniewski A, Mory F, et al. A soluble form of the triggering receptor expressed on myeloid cells-1 modulates the inflammatory response in murine sepsis. *J Exp Med.* 2004;200(11):1419-26.
14. Caer C, Gorreja F, Forsskahl SK, Brynjolfsson SF, Szeponik L, Magnusson MK, et al. TREM-1+ Macrophages Define a Pathogenic Cell Subset in the Intestine of Crohn's Disease Patients. *J Crohns Colitis.* 2021;15(8):1346-61.
15. Che X, Park KC, Park SJ, Kang YH, Jin HA, Kim JW, et al. Protective effects of guggulsterone against colitis are associated with the suppression of TREM-1 and modulation of macrophages. *Am J Physiol Gastrointest Liver Physiol.* 2018;315(1):G128-G39.
16. Amrun SN, Tan JJL, Rickett NY, Cox JA, Lee B, Griffiths MJ, et al. TREM-1 activation is a potential key regulator in driving severe pathogenesis of enterovirus A71 infection. *Sci Rep.* 2020;10(1):3810.

17. Campanholle G, Mittelsteadt K, Nakagawa S, Kobayashi A, Lin SL, Gharib SA, et al. TLR-2/TLR-4 TREM-1 signaling pathway is dispensable in inflammatory myeloid cells during sterile kidney injury. *PLoS One.* 2013;8(7):e68640.
18. Ornatowska M, Azim AC, Wang X, Christman JW, Xiao L, Joo M, et al. Functional genomics of silencing TREM-1 on TLR4 signaling in macrophages. *Am J Physiol Lung Cell Mol Physiol.* 2007;293(6):L1377-84.
19. Bhattacharyya S, Wang W, Qin W, Cheng K, Coulup S, Chavez S, et al. TLR4-dependent fibroblast activation drives persistent organ fibrosis in skin and lung. *JCI Insight.* 2018;3(13).
20. Bhattacharyya S, and Varga J. Endogenous ligands of TLR4 promote unresolving tissue fibrosis: Implications for systemic sclerosis and its targeted therapy. *Immunol Lett.* 2018;195:9-17.
21. Joffre J, Potteaux S, Zeboudj L, Loyer X, Boufenzer A, Laurans L, et al. Genetic and Pharmacological Inhibition of TREM-1 Limits the Development of Experimental Atherosclerosis. *J Am Coll Cardiol.* 2016;68(25):2776-93.
22. Lemarie J, Boufenzer A, Popovic B, Tran N, Groubatch F, Derive M, et al. Pharmacological inhibition of the triggering receptor expressed on myeloid cells-1 limits reperfusion injury in a porcine model of myocardial infarction. *ESC Heart Fail.* 2015;2(2):90-9.
23. Xiong JB, Duan JX, Jiang N, Zhang CY, Zhong WJ, Yang JT, et al. TREM-1 exacerbates bleomycin-induced pulmonary fibrosis by aggravating alveolar epithelial cell senescence in mice. *Int Immunopharmacol.* 2022;113(Pt A):109339.
24. Siskind S, Royster W, Brenner M, and Wang P. A novel eCIRP/TREM-1 pathway inhibitor attenuates acute kidney injury. *Surgery.* 2022;172(2):639-47.
25. Francois B, Lambden S, Fivez T, Gibot S, Derive M, Grouin JM, et al. Prospective evaluation of the efficacy, safety, and optimal biomarker enrichment strategy for nangibotide, a TREM-1 inhibitor, in patients with septic shock (ASTONISH): a double-blind, randomised, controlled, phase 2b trial. *Lancet Respir Med.* 2023;11(10):894-904.
26. Ajith A, Mamouni K, Horuzsko DD, Musa A, Dzutsev AK, Fang JR, et al. Targeting TREM1 augments antitumor T cell immunity by inhibiting myeloid-derived suppressor cells and restraining anti-PD-1 resistance. *J Clin Invest.* 2023;133(21).
27. Brynjolfsson SF, Magnusson MK, Kong PL, Jensen T, Kuijper JL, Hakansson K, et al. An Antibody Against Triggering Receptor Expressed on Myeloid Cells 1 (TREM-1) Dampens Proinflammatory Cytokine Secretion by Lamina Propria Cells from Patients with IBD. *Inflamm Bowel Dis.* 2016;22(8):1803-11.
28. Sigalov AB. SCHOOL of nature: ligand-independent immunomodulatory peptides. *Drug Discov Today.* 2020;25(8):1298-306.
29. Siskind S, Brenner M, and Wang P. TREM-1 Modulation Strategies for Sepsis. *Front Immunol.* 2022;13:907387.
30. Gibot S, Buonsanti C, Massin F, Romano M, Kolopp-Sarda MN, Benigni F, et al. Modulation of the triggering receptor expressed on the myeloid cell type 1 pathway in murine septic shock. *Infect Immun.* 2006;74(5):2823-30.
31. Gibot S, Massin F, Marcou M, Taylor V, Stidwill R, Wilson P, et al. TREM-1 promotes survival during septic shock in mice. *Eur J Immunol.* 2007;37(2):456-66.
32. Francois B, Wittebole X, Ferrer R, Mira JP, Dugernier T, Gibot S, et al. Nangibotide in patients with septic shock: a Phase 2a randomized controlled clinical trial. *Intensive Care Med.* 2020;46(7):1425-37.
33. Bruno François XW, Ricard Ferrer, Jean-Paul Mira, Thierry Dugernier, Sébastien Gibot, Marc Derive, Peter Pickkers, Jean-Jacques Garaud, Miguel Sanchez, Margarita Salcedo-Magguilli, Pierre-François Laterre. P1 Safety and pharmacodynamic activity of a novel TREM-1 pathway inhibitory

peptide in septic shock patients: phase IIa clinical trial results. *Intensive Care Med Exp.* 2018;6(Suppl 1):1-33.

34. Derive M, Boufenzer A, Bouazza Y, Groubatch F, Alauzet C, Barraud D, et al. Effects of a TREM-like transcript 1-derived peptide during hypodynamic septic shock in pigs. *Shock.* 2013;39(2):176-82.
35. Cuvier V, Lorch U, Witte S, Olivier A, Gibot S, Delor I, et al. A first-in-man safety and pharmacokinetics study of nangibotide, a new modulator of innate immune response through TREM-1 receptor inhibition. *Br J Clin Pharmacol.* 2018;84(10):2270-9.
36. Shen ZT, and Sigalov AB. Novel TREM-1 Inhibitors Attenuate Tumor Growth and Prolong Survival in Experimental Pancreatic Cancer. *Mol Pharm.* 2017;14(12):4572-82.
37. Rojas MA, Shen ZT, Caldwell RB, and Sigalov AB. Blockade of TREM-1 prevents vitreoretinal neovascularization in mice with oxygen-induced retinopathy. *Bba-Mol Basis Dis.* 2018;1864(9):2761-8.
38. Tornai D, Furi I, Shen ZT, Sigalov AB, Coban S, and Szabo G. Inhibition of Triggering Receptor Expressed on Myeloid Cells 1 Ameliorates Inflammation and Macrophage and Neutrophil Activation in Alcoholic Liver Disease in Mice. *Hepatol Commun.* 2019;3(1):99-115.
39. Sigalov AB. Inhibition of TREM-2 Markedly Suppresses Joint Inflammation and Damage in Experimental Arthritis. *Int J Mol Sci.* 2022;23(16).
40. Bale S, Verma P, Yalavarthi B, Scarneo SA, Hughes P, Amin MA, et al. Pharmacological inhibition of TAK1 prevents and induces regression of experimental organ fibrosis. *JCI Insight.* 2023;8(14).
41. Xu P, Zhang X, Liu Q, Xie Y, Shi X, Chen J, et al. Microglial TREM-1 receptor mediates neuroinflammatory injury via interaction with SYK in experimental ischemic stroke. *Cell Death Dis.* 2019;10(8):555.
42. Varga J, and Abraham D. Systemic sclerosis: a prototypic multisystem fibrotic disorder. *J Clin Invest.* 2007;117(3):557-67.
43. Toledo DM, and Pioli PA. Macrophages in Systemic Sclerosis: Novel Insights and Therapeutic Implications. *Curr Rheumatol Rep.* 2019;21(7):31.
44. Volkmann ER, Andreasson K, and Smith V. Systemic sclerosis. *Lancet.* 2023;401(10373):304-18.
45. Tomita H, Ogawa F, Hara T, Yanaba K, Iwata Y, Muroi E, et al. Elevated Serum Concentrations of Triggering Receptor Expressed on Myeloid Cells-1 in Diffuse Cutaneous Systemic Sclerosis: Association with Severity of Pulmonary Fibrosis. *J Rheumatol.* 2010;37(4):787-91.
46. Dang SC, Shen Y, Yin K, and Zhang JX. TREM-1 Promotes Pancreatitis-Associated Intestinal Barrier Dysfunction. *Gastroent Res Pract.* 2012;2012.
47. Gibot S, Massin F, Alauzet C, Derive M, Montemont C, Collin S, et al. Effects of the Trem 1 Pathway Modulation during Hemorrhagic Shock in Rats. *Shock.* 2009;32(6):633-7.
48. Schenk M, Bouchon A, Seibold F, and Mueller C. TREM-1-expressing intestinal macrophages crucially amplify chronic inflammation in experimental colitis and inflammatory bowel diseases. *J Clin Invest.* 2007;117(10):3097-106.
49. Kuai J, Gregory B, Hill A, Pittman DD, Feldman JL, Brown T, et al. TREM-1 expression is increased in the synovium of rheumatoid arthritis patients and induces the expression of pro-inflammatory cytokines. *Rheumatology.* 2009;48(11):1352-8.
50. Weber B, Schuster S, Zysset D, Rihs S, Dickgreber N, Schürch C, et al. TREM-1 Deficiency Can Attenuate Disease Severity without Affecting Pathogen Clearance. *Plos Pathog.* 2014;10(1).
51. Arts RJ, Joosten LA, van der Meer JW, and Netea MG. TREM-1: intracellular signaling pathways and interaction with pattern recognition receptors. *J Leukoc Biol.* 2013;93(2):209-15.
52. Bhattacharyya S, Midwood KS, Yin H, and Varga J. Toll-Like Receptor-4 Signaling Drives Persistent Fibroblast Activation and Prevents Fibrosis Resolution in Scleroderma. *Adv Wound Care (New Rochelle).* 2017;6(10):356-69.

53. Shen ZT, and Sigalov AB. Rationally designed ligand-independent peptide inhibitors of TREM-1 ameliorate collagen-induced arthritis. *J Cell Mol Med.* 2017;21(10):2524-34.
54. Wang W, Bale S, Wei J, Yalavarthi B, Bhattacharyya D, Yan JJ, et al. Fibroblast A20 governs fibrosis susceptibility and its repression by DREAM promotes fibrosis in multiple organs. *Nat Commun.* 2022;13(1):6358.
55. Wang W, Bale S, Yalavarthi B, Verma P, Tsou PS, Calderone KM, et al. Deficiency of inhibitory TLR4 homolog RP105 exacerbates fibrosis. *JCI Insight.* 2022;7(21).

FIGURES

Figure 1

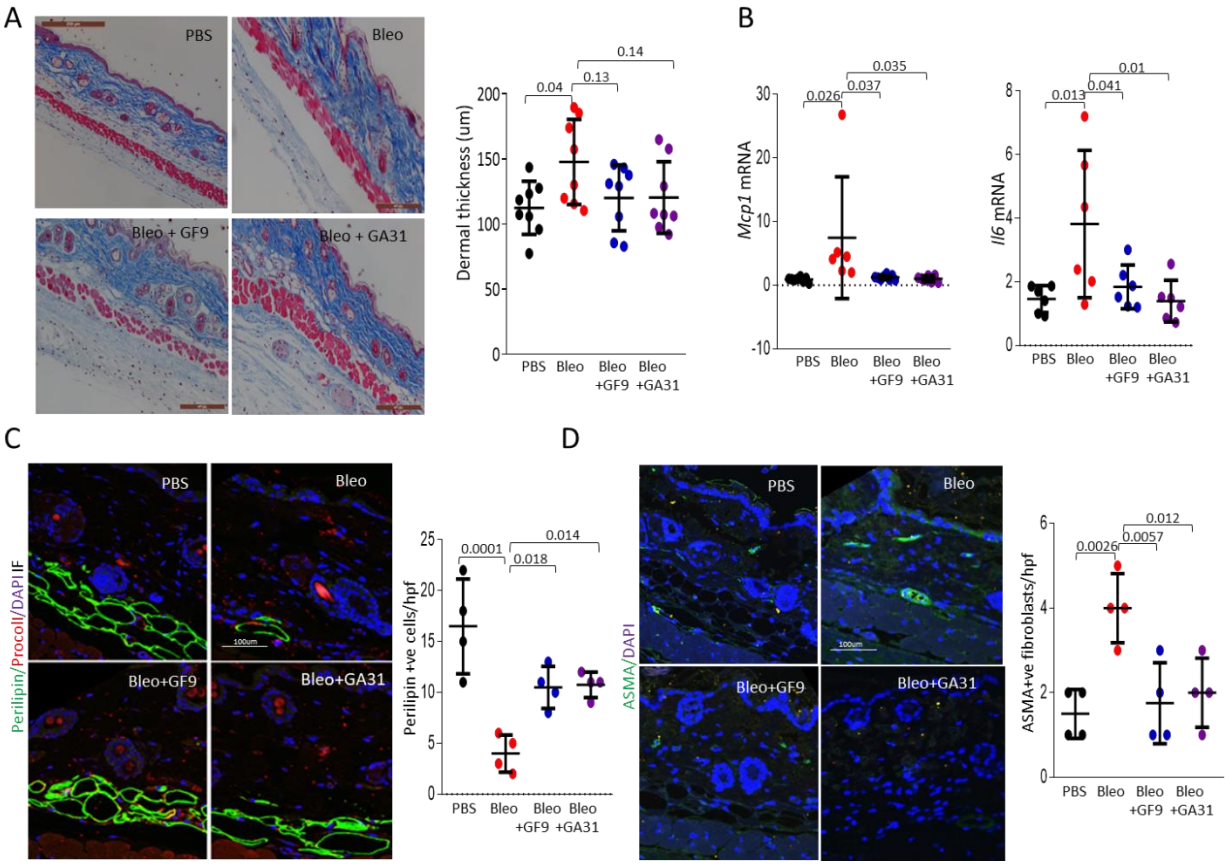

Figure 1: Pharmacological inhibition of TREM-1 prevents early loss of dermal adipose tissue

C57/BL6 mice received daily s.c. injections of PBS or bleomycin alone, or together with GF9 and GA31-LPC or vehicle for 5 days. Mice were sacrificed on day 8 and skin was harvested for analysis. **A.** Trichrome stains, representative images. Bar-100 μm (left panel); dermal thickness (right panel, means ± SD of eight determinations/hpf). One-way analysis of variance followed by Sidak's multiple comparison. **B.** Real-time quantitative PCR. Results, normalized with GAPDH,

are means ±s.d. of triplicate determinations from six mice per group; One-way analysis of variance followed by Sidak's multiple comparison test. **C.** Immunolabelling using antibodies to perilipin (green), procollagen I (red) and DAPI (blue). Representative images. Bar = 100 µm. **D.** Antibodies to ASMA (green) and DAPI (blue). ASMA positive cells (average from four randomly selected from four mice/group). One-way analysis of variance followed by Sidak's multiple comparisons test.

Figure 2

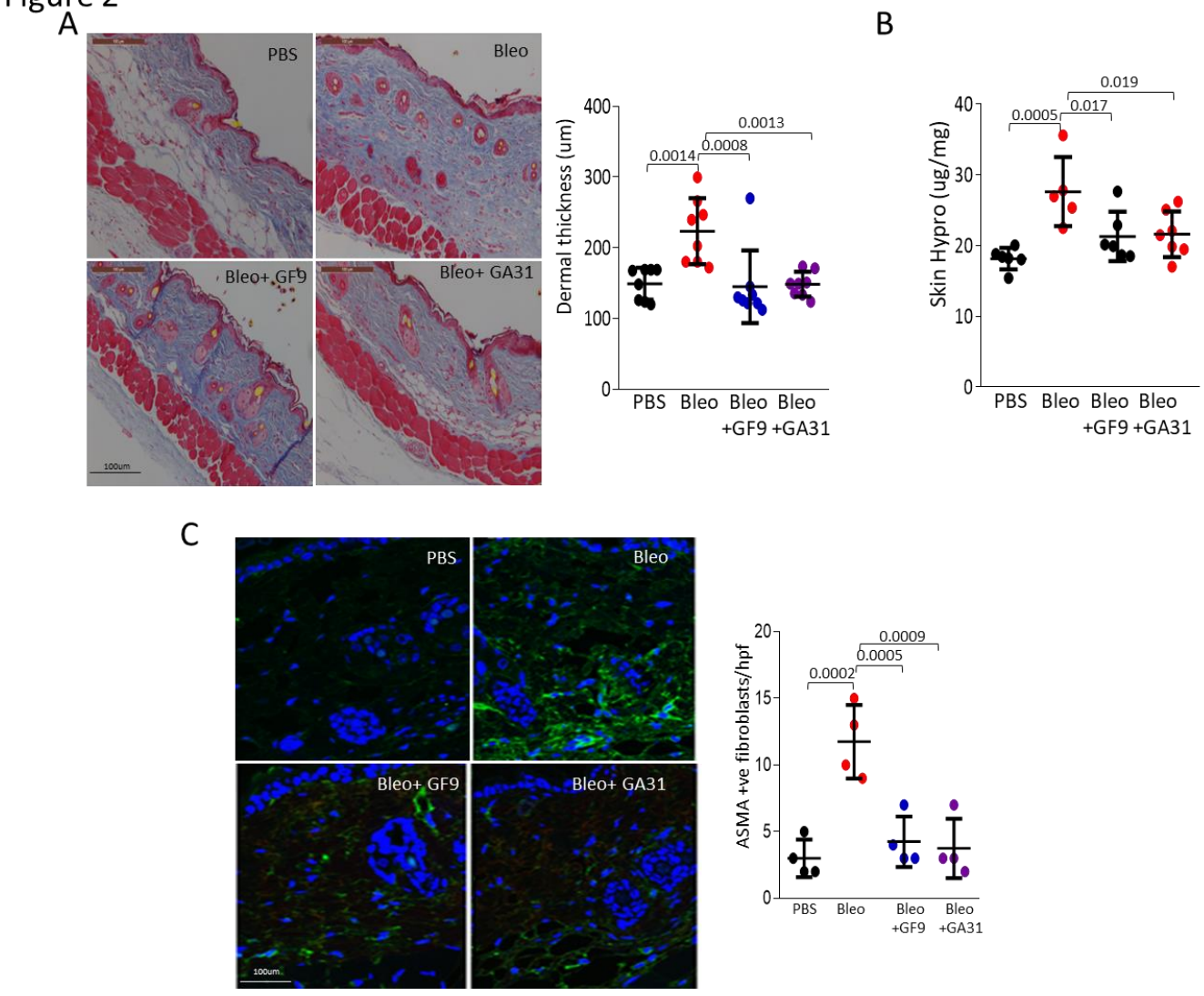

Figure 2: Inhibition of TREM-1 signaling by GA31-LPC treatment prevents skin fibrosis.

C57/BL6 mice were treated as described in Fig1 above and were sacrificed on day 22 and skin was harvested for analysis. **A.** Trichrome stains, representative images, bar-100 µm (left panel); dermal thickness (right panel, means ± SD of eight determinations/hpf). One-way analysis of variance followed by Sidak's multiple comparisons test. **B.** Skin hydroxyproline assays; results are mean ± SEM. **C.** Immunolabelling using antibodies to ASMA (green) and DAPI (blue). Representative images. Bar = 100 µm. ASMA-positive cells (average from four randomly selected from four mice/group). One-way analysis of variance followed by Sidak's multiple comparisons test.

Figure 3

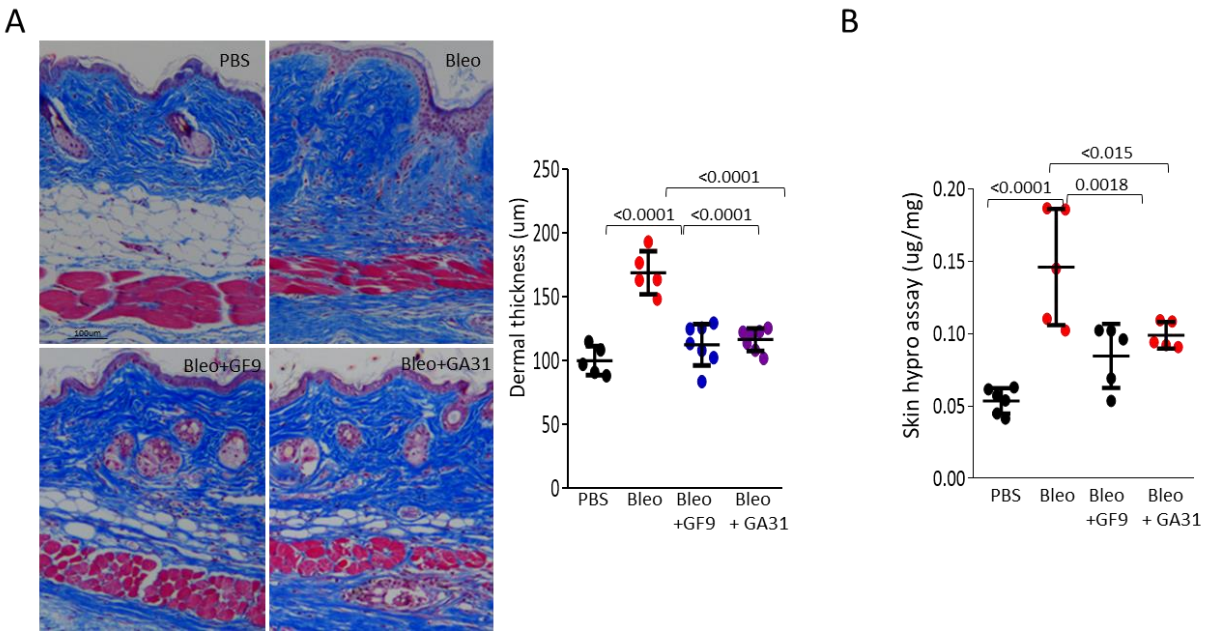

Figure 3: Inhibition of TREM-1 signaling by GF9 and GA31-LPC treatment mitigates established skin fibrosis.

C57/BL6 mice were randomized to four treatment groups (n=5-8 mice/group), euthanized on day 28 and skin was harvested. **A.** Trichrome stains, representative images, bar-100 µm (left panel); dermal thickness (right panel, means ± SD of five to eight determinations/hpf). One-way analysis

of variance was followed by Sidak's multiple comparisons test. **B.** Hydroxyproline assays, One-way analysis of variance followed by Sidak's multiple comparisons test.

Figure 4

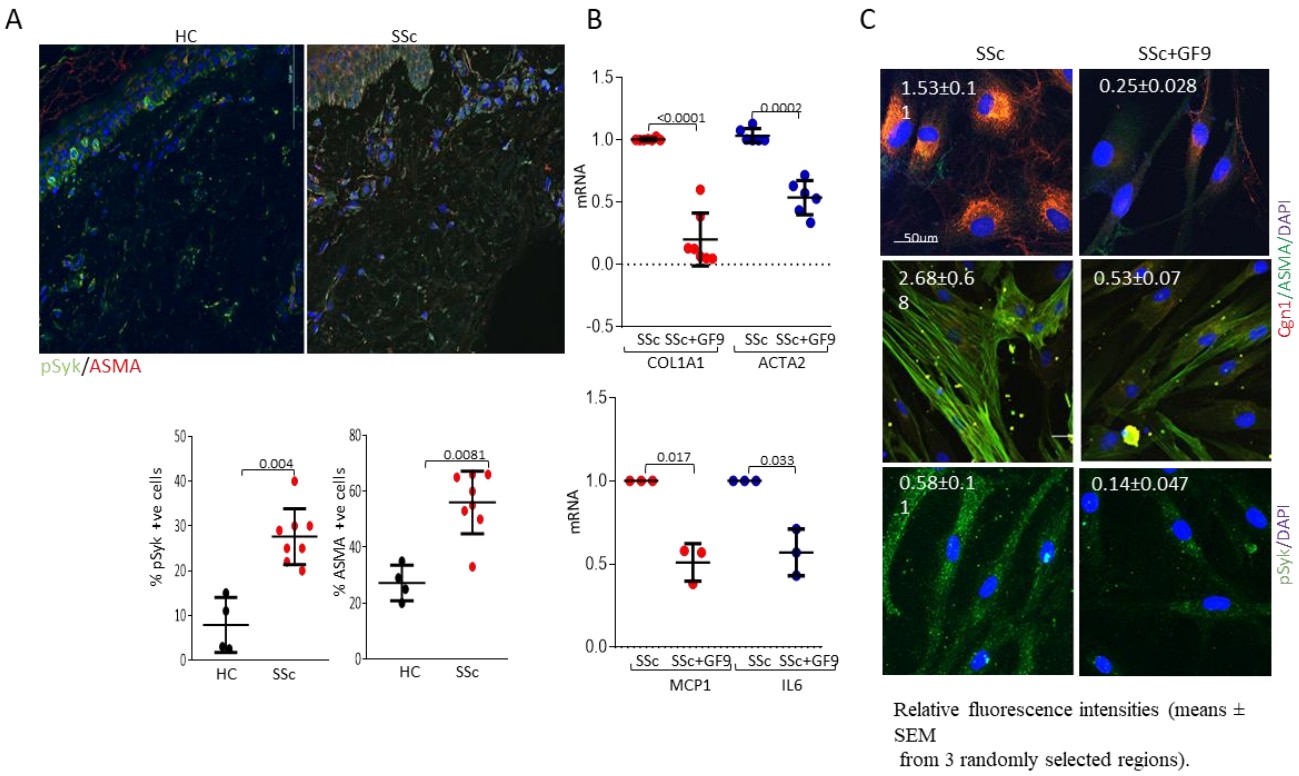

Figure 4: TREM-1 signaling is activated in SSc skin.

A. Skin biopsies from patients with SSc (n=8) and healthy controls (n=4) were immunolabeled with antibodies to phospho-Syk or ASMA, and immunofluorescence was visualized by Nikon A1R laser scanning confocal microscope; the percentage of immunopositive cells (means from four randomly selected regions) were quantified. Mann-Whitney U test. B. Confluent SSc skin fibroblasts (n=8, upper panel; n=3, lower panel) were incubated with GF9 for 24 h, and mRNA levels were quantitated by real-time quantitative PCR. Results, normalized with GAPDH, are means±s.d. of triplicate determinations from individual patient. Paired t test. C. SSc fibroblasts

(n=6) were immunolabeled using antibodies to collagen I, ASMA or pSyk (bar-100µm). Representative images. Relative fluorescence intensities (means ± SEM from 3 randomly selected regions).

SUPPLEMENTARY FIGURE

Suppl. Figure 1

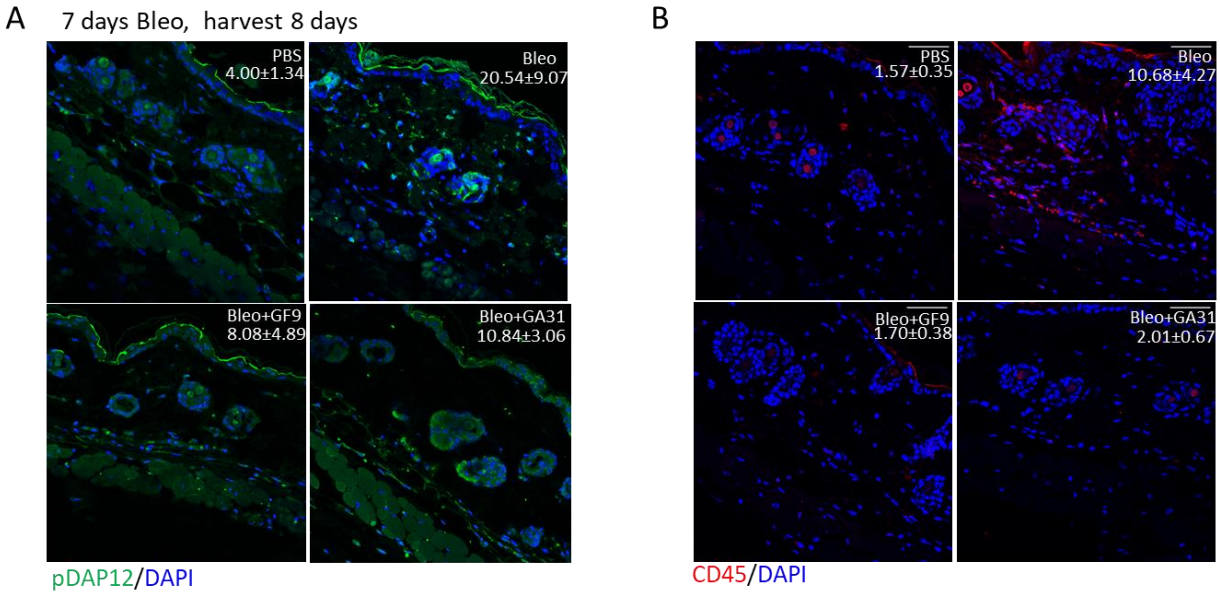

Supplementary Figure 1. **Inhibition of TREM-1 signaling by GF9 and GA31-LPC treatment attenuated pDAP12 and CD45 levels in mice skin tissue**. C57/BL6 mice received daily s.c. injections of PBS or bleomycin alone, or together with GF9 and GA31-LPC or vehicle. Mice were sacrificed on day 8. Skin tissues for the respective groups were immunolabelled with antibodies to (A) pDAP12 and (B) CD45 (bar, 50 µm). Quantitation of pDAP12 and CD45 positive cells (means ± SD; average from three randomly selected from four mice/group). Representative images.

Suppl. Figure 2

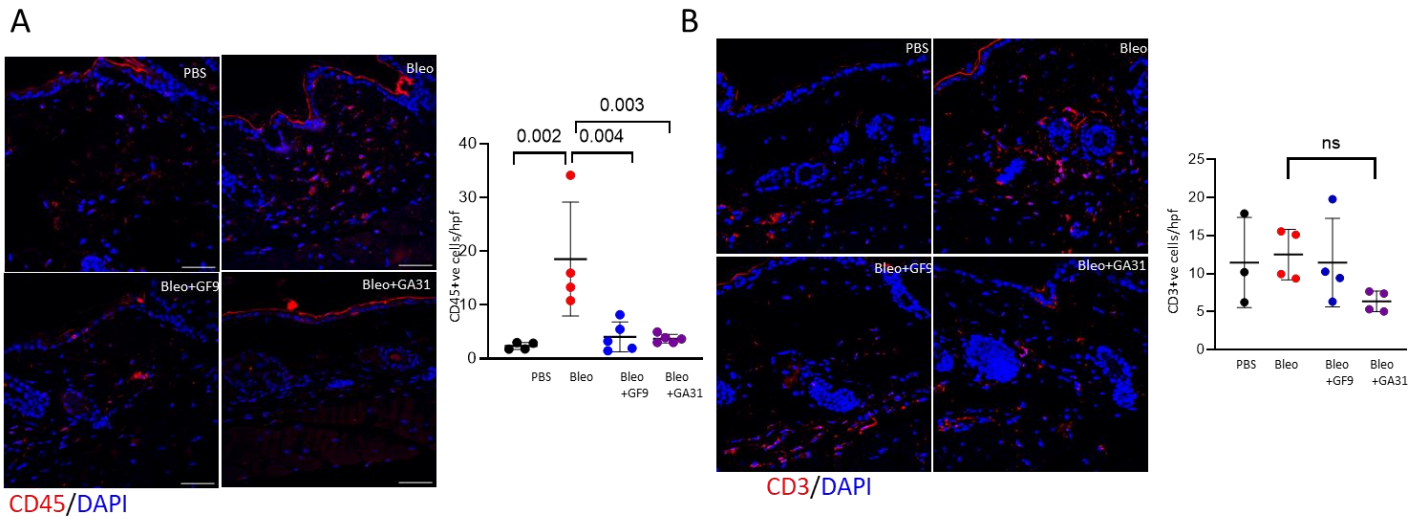

Supplementary Figure 2. **GF9 and GA31-LPC concomitant treatment with bleomycin attenuated immune cell infiltrations.** C57/BL6 mice received daily s.c. injections of PBS or bleomycin alone, or together with GF9 and GA31-LPC or vehicle. Mice were sacrificed on day 22. Skin tissues for the respective groups were immunolabelled with antibodies to A) CD45 for leukocytes and B) CD3 for T-lymphocytes (left panel, representative images, bar, 50μm) with quantification (right panel).

Suppl. Figure 3

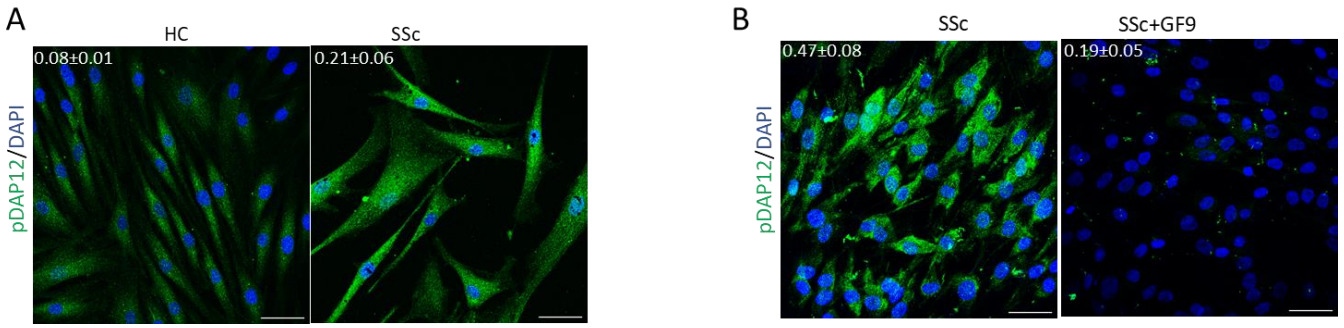

Supplementary Figure 3. TREM-1 downstream target is activated in SSc fibroblast. A. HC (n=2) and SSc fibroblasts (n=2) were immunolabeled using antibodies to pDAP12 (bar-50μm) and visualized by Nikon A1R laser scanning confocal microscope. Representative images. Relative fluorescence intensities (means ± SEM from 3 randomly selected regions). B. Confluent SSc skin fibroblasts (n=3, were incubated with GF9 for 24 h, and immunolabeled using antibodies to pDAP12 (bar-100μm). Representative images. Relative fluorescence intensities (means ± SEM from 3 randomly selected regions).

Suppl. Figure 4

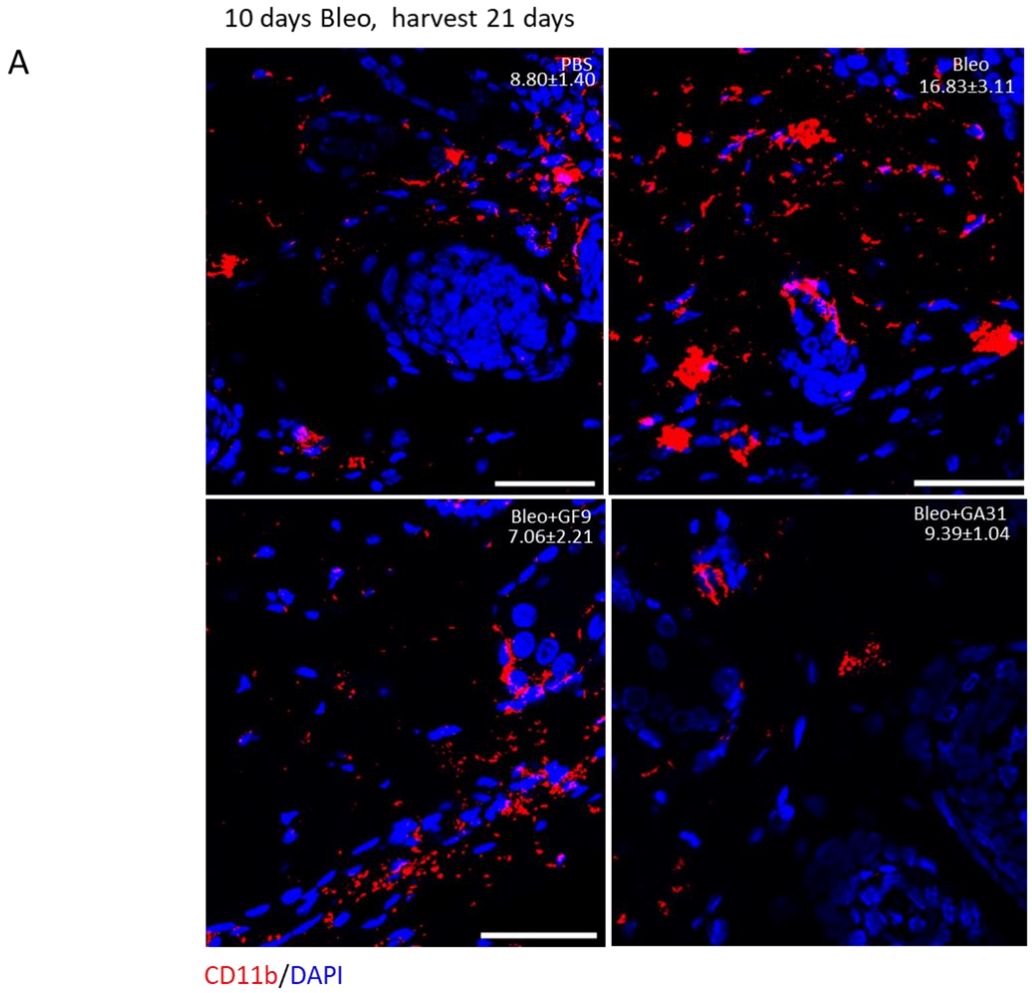

Supplementary Figure 4. **GF9 and GA31-LPC concomitant treatment with bleomycin attenuated myeloid cell infiltrations.** C57/BL6 mice received daily s.c. injections of PBS or bleomycin alone, or together with GF9 and GA31-LPC or vehicle. Mice were sacrificed on day 22. Skin tissues for the respective groups were immunolabelled with antibodies to A) CD11b for myeloid cells (representative images, bar, 50µm) with quantification (right panel). Quantitation of CD11b positive cells (means ± SEM; average from three randomly selected from four mice/group).

Table 1 Clinical characteristics of subjects (skin biopsies used to establish explanted fibroblast lines)

Identity	Age (years)	Sex	Ethnicity	SSc	Subtype	Disease duration
SAPRC_SSc_7	50	Female	White	Non-hispanic	Diffuse	8.96 months
SAPRC_SSc_11	64	Female	White	Non-hispanic	Diffuse	8.24 months
SAPRC_SSc_31	60	Female	White	Non-hispanic	Diffuse	12.8 months
SAPRC_SSc_37	63	Female	White	Non-hispanic	Diffuse	13.07 months
SAPRC_SSc_40	43	Female	White	Non-hispanic	Diffuse	9.16 months
SAPRC_SSc_43	55	Female	Black	Non-hispanic	Diffuse	11.20 months
SAPRC_SSc_44	64	Female	White	Non-hispanic	Diffuse	7.16 months
SAPRC_SSc_45	62	Female	White	Non-hispanic	Diffuse	19.44 months

Table 2 -List of primers used for gene expression.

hIL-6-F	AAATTCGGTACATCCTCGACGG
hIL-6-R	GGAAGGTTCAGGTTGTTTTCTGC
hACTA2-F	CAGGGCTGTTTTCCCATCCAT
hACTA2-R	GCCATGTTCTATCGGGTACTTC
hCOL1A1-F	CTGAGTCAGCAGATTGAGAACA
hCOL1A1-R	AGGTTGCAGCCTTGGTTAG
hGAPDH-F	CATGAGAAGTATGACAACAGCCT
hGAPDH-R	AGTCCTTCCACGATACCAAAGT
hMCP1-F	ACTGAAGCTCGTACTCTC
hMCP1-R	CTTGGGTTGTGGAGTGAG
mMCP1-F	CATCCACGTGTTGGCTCA
mMCP1-R	GATCATCTTGCTGGTGAATGAGT
mGAPDH-F	ATCTTCTTGTGCAGTGCCAGC
mGAPDH-R	GTTGATGGCAACAATCTCCAC
mIL-6-F	GAGGATACCACTCCCAACAGACC
mIL-6-R	AAGTGCATCATCGTTCATACA